Engineering Structures 42 (2012) 201–213

Contents lists available at SciVerse ScienceDirect

Engineering Structures

journal homepage: www.elsevier.com/locate/engstruct

Multi-phase modelling of ionic transport in concrete when subjected to an externally applied electric field

Qing-feng Liu [a], Long-yuan Li [a,*], Dave Easterbrook [a], Jian Yang [b]

[a] School of Marine Science and Engineering, University of Plymouth, Plymouth PL4 8AA, UK
[b] School of Civil Engineering, University of Birmingham, Birmingham B15 2TT, UK

ARTICLE INFO

Article history:
Received 28 January 2012
Revised 23 April 2012
Accepted 26 April 2012
Available online 1 June 2012

Keywords:
Corrosion
Chloride
Migration
Concrete
Cement
Multi-phase
Ionic interaction

ABSTRACT

Chloride-induced reinforcing steel corrosion is a worldwide problem. In order to predict how chlorides penetrate in concrete and how other ionic species in concrete pore solution affect the penetration of chlorides, this paper presents a numerical study on the two-phase modelling of ionic transport in concrete when subjected to an externally applied electric field. In most existing work, researchers tend to use the assumption of electro-neutrality condition to determine the electrostatic potential within an electrolyte in one-dimensional problems and consider only one phase. In contrast, this study employed a two-phase numerical model of concrete and the Poisson's equation for determining the electrostatic potential. By solving both mass conservation and Poisson's equations, the distribution profiles of each ionic species and electrostatic potential at any required time were successfully obtained. The results obtained from the present two-phase modelling reveal some important features which cannot be found from existing one-dimensional and one-phase models.

1. Introduction

It is well known that the ingression of ions, especially the chloride ions, in concrete will cause serious corrosion problems for reinforcing steel in concrete structures. Thus, the investigation of transport of ionic species in concrete is very important and has received great attention in past decades. Apart from the experimental studies, there are also analytical and numerical studies aiming to characterise the transport behaviour of ionic species in cement and/or concrete materials.

In the analytical study, there are a number of publications which have been focussed on clarifying the diffusion coefficient on the basis of different scales. At the macroscopic level, the analytical method brings some empirical models. It was revealed from these models that the diffusion coefficient tends to have a connection with the water to cement ratio [1,2]. In the work of Dormieux and Lemarchand [3], Garboczi [4], Brakel and Heertjes [5], Xu et al. [6], Li and Xia [7] the relationship between diffusion coefficient and the conception of porosity and tortuosity was discussed at a microscopic level. In contrast to microscopic models, the mesoscopic models consider the components of the two or three phases (aggregate and cement matrix; aggregate, bulk cement paste and interfacial transition zone) and their corresponding diffusive properties respectively in these different phases [8,9]. However, all of the models mentioned above focus only on the ionic transport of a single-species, i.e. the chloride ions.

Great efforts have been made on the assessment of ionic transport by using experimental techniques. For ionic diffusion, there are two common test methods which were often used for measuring the chlorides' penetration in concrete. One is the salt ponding test (AASHTO T259 [10]) and the other is the bulk diffusion test (Nordtest NTBuild 443 [11]). However, these two diffusion tests are very time-consuming, especially for high-performance concrete, of which the test duration may last 90 days or even longer in order to get a sufficient chloride profile. Hence, people tend to adopt alternative experiments based on electro-migration of ions, which include the rapid chloride permeability test and the rapid migration test.

The rapid chloride permeability test, undertaken by gauging the electrical conductivity or resistance of concrete directly or indirectly, was initially presented by Whiting [12] and then adopted as AASHTO T277 [13] and ASTM C1202 [14]. The main drawback of this method is that the results obtained from electrical conductivity or resistance measurement cannot exactly represent the permeability, since the permeability of concrete attributes to its pore structure, whereas the electrical conductivity or resistance depends on not only the pore structure but also the chemistry of the pore solution. This deviation will be even higher when acting on concrete made with fly ash, siliceous dust and other super-plasticizer admixture. To examine this method,

* Corresponding author. Tel.: +44 1752 586 180; fax: +44 1752 586 101.
E-mail address: long-yuan.li@plymouth.ac.uk (L.-y. Li).

0141-0296/$ - see front matter © 2012 Elsevier Ltd. All rights reserved.
http://dx.doi.org/10.1016/j.engstruct.2012.04.021

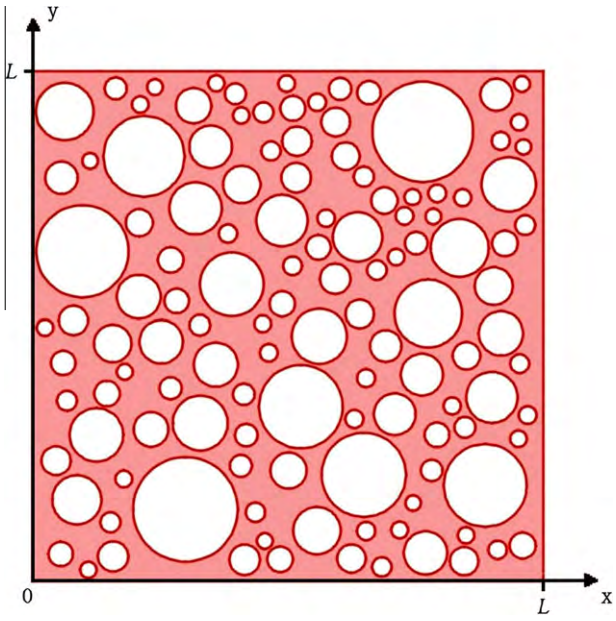

Fig. 1. Two-dimensional model: section of concrete, $(1-\phi)=0.5$.

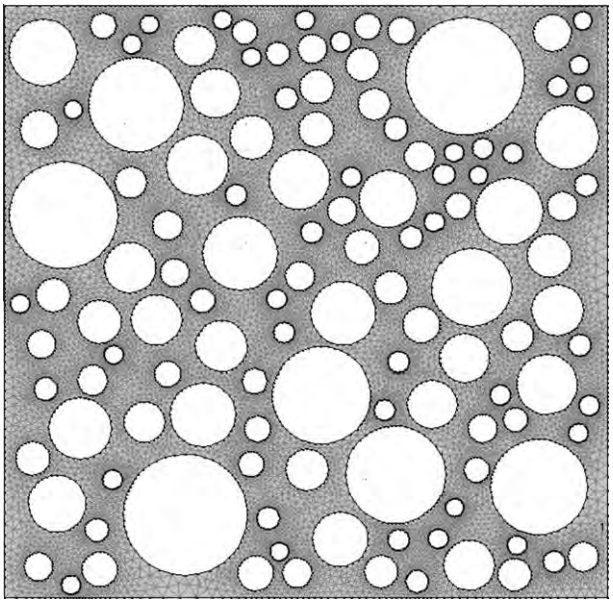

Fig. 3. Finite element mesh (circular shape of aggregates) volume fraction $(1-\phi)=0.5$.

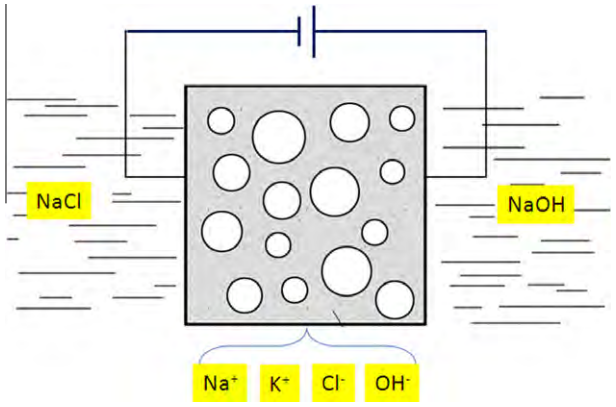

Fig. 2. Schematic representation of a migration test.

Andrade [15] employed a migration test and indicated that the function between measured charge through the concrete and the moving ions is more suitable for hydroxyls than chlorides. A comparison made by Pfeifer et al. [16] also showed that the rapid chloride permeability test result is unreliable.

The rapid migration test was developed by Tang and Nilsson [17] and adopted by Nordtest and AASHTO as NT Build 492 and provisional Standard TP64 [18]. The test is very similar with the rapid chloride permeability test. However, it allows direct measurement by the depth of chloride penetration instead of using the total passed charge to estimate the permeability. The calculation of chloride diffusion coefficient in the rapid migration test requires the concentration of chlorides at the depth they penetrated, which is often difficult to obtain. In current practice it usually uses the surface chloride concentration, which means that the penetration of chlorides in concrete exactly follows the one-dimensional migration pattern. The relevance between the chloride migration rate and the electrical current obtained from a given voltage charge passed in the steady state was reported by Yang and Cho [19].

Nevertheless, the experimental data in the literature were mostly obtained by means of taking traditional concrete as a specimen while very few were for the new types of concrete (involving various kinds of additives). Additionally, similar to analytical methods, these test approaches are only used to investigate the transport of just a single ionic species, i.e. chloride ions, in one time.

Since the analytical techniques usually take simple cases and are difficult in dealing with interactions between different ionic species and the electrostatic coupling of ions in a multi-component electrolyte solution, researchers began to use numerical methods to investigate the transport behaviour of multi-species in concrete. Methodologically speaking, these works can be divided into four categories. Firstly, a series of studies [20–23] established numerical models to simulate the penetration process through a saturated cement paste under the hypothesis of zero current and electro-neutrality condition. Secondly, there were also some works other than the above ones, which added the effect of externally applied current density as well as considering the interactions between ionic

Table 1
Boundary conditions, initial conditions and diffusion coefficients.

Field variables		Potassium (mol/m^3)	Sodium (mol/m^3)	Chloride (mol/m^3)	Hydroxide (mol/m^3)	Electrostatic potential (V)
Boundary conditions	$x=0$	0	520	520	0	$\Phi=0$
	$x=L$	0	300	0	300	$\Phi=24$
	$y=0$	$J=0$	$J=0$	$J=0$	$J=0$	$\partial\Phi\partial y=0$
	$y=L$	$J=0$	$J=0$	$J=0$	$J=0$	$\partial\Phi\partial y=0$
Initial conditions		200	100	0	300	0
Charge number		1	1	−1	−1	N/A
Apparent diffusion coefficient, $\times10^{-10}$ m^2/s		1.957	1.334	2.032	5.260	N/A

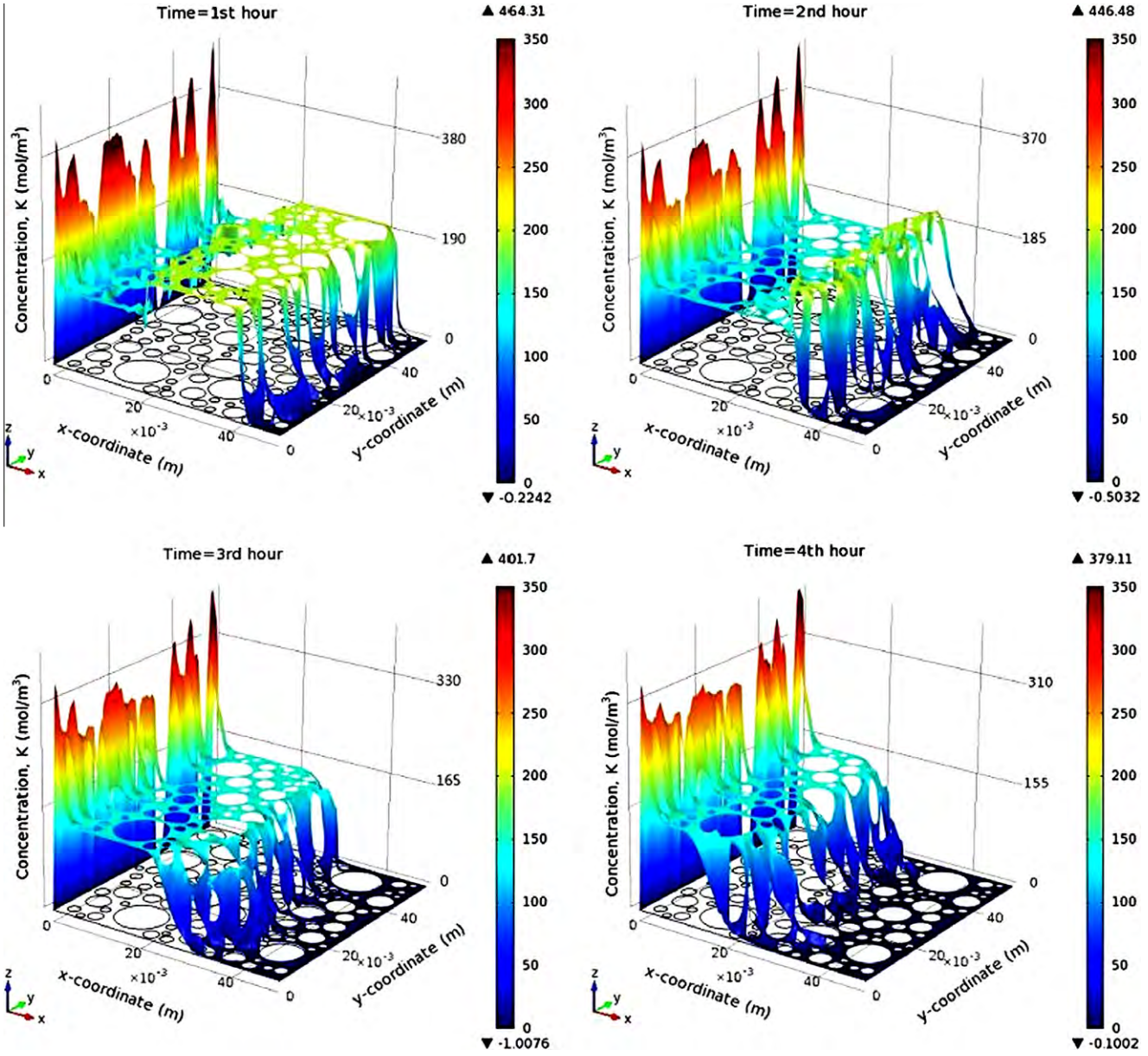

Fig. 4. Concentration distribution profiles of potassium ions.

species during the transport of ionic species in cement-based porous materials [24–36]. Also, in these studies, the electrostatic potential throughout the electrochemical process was still controlled by assuming the electro-neutrality condition. Similarly, Friedmann et al. [37], Krabbenhoft and Krabbenhoft [38], Narsillo et al. [39] utilised externally applied voltage instead of the external current density as adopted in the second category. Here, it should be pointed out that, the electro-neutrality condition, which is employed in the work mentioned above to govern the electrostatic potential at any point in an electrolyte solution, is not a constitutive law but only a mathematical approximation in the electrochemistry field and may cause numerical inaccuracy. The real constitutive law for governing the electrostatic potential is the Poisson equation (will be showed in the next session). However, some numerical difficulty exists in solving the Poisson equation because of the large and small numbers involved in the equation. More recently, Johannesson et al. [40–43] conducted a series of studies for exploring the ionic diffusion in a multi-component solution by using the Poisson equation instead of the electro-neutrality condition. However, these studies did not involve external voltage. Hence, the transport of ions in those cases is actually still dominated by diffusion, whereas the migration occurred only because of the imbalance diffusion between different ionic species.

In this paper, a numerical investigation is conducted, which employs not only the Poisson equation but also an external electric field to control the ionic transport in a multi-component solution within a saturated concrete. In view that most previous numerical models considered only one-dimensional and one-phase problems, this study established a two-phase numerical model of concrete to simulate the ionic transport process. By solving both mass conservation and Poisson's equations, the distribution profiles of four involved ionic species (potassium, sodium, chloride, and hydroxide) and electrostatic potential at any required time were successfully obtained. Also, through the two-dimensional and two-phase numerical model, we have found some important interaction transport features between ionic species which have not been seen before in the one-dimensional model of single phase.

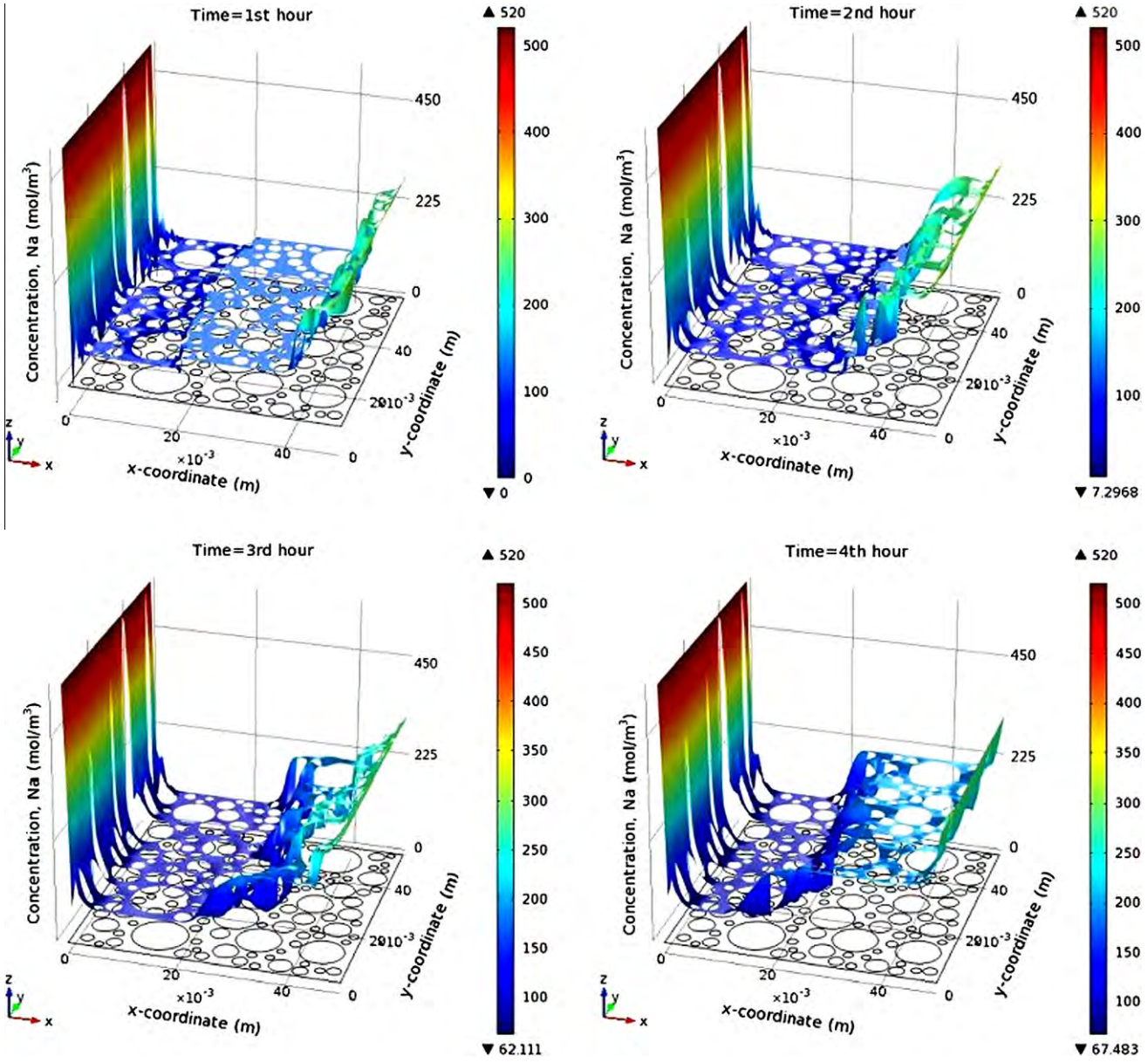

Fig. 5. Concentration distribution profiles of sodium ions.

2. Theoretical background

By using the assumption that the concrete is a saturated pore medium and there are no chemical reactions between ionic species occurring in both liquid and solid phases, the following mass conservation for each individual ionic species involved in the concrete can be obtained:

$$\frac{\partial C_k}{\partial t} = -\nabla J_k \qquad k = 1, \cdots, N \tag{1}$$

where C_k is the concentration of the kth ionic species, t is the time, J_k is the flux of the kth ionic species, and N is the total number of the ionic species contained in the concrete. Diffusion and migration are treated as the major reason for ionic transport in this study; therefore, the ionic flux equation can be expressed as follows:

$$J_k = -D_k \nabla C_k - D_k C_k \frac{z_k F}{RT} \nabla \Phi \qquad k = 1, \cdots, N \tag{2}$$

where D_k and z_k are the diffusion coefficient and the charge number of the kth ionic species, respectively, $F = 9.648 \times 10^{-4}$ C mol^{-1} is the Faraday constant, $R = 8.314$ J mol^{-1} K^{-1} is the ideal gas constant, $T = 298$ K is the absolute temperature, Φ is the electrostatic potential. Substituting Eq. (2) into (1), yields:

$$\frac{\partial C_k}{\partial t} = \nabla(D_k \nabla C_k) + \frac{z_k D_k F}{RT} \nabla(C_k \nabla \Phi) \qquad k = 1, \cdots, N \tag{3}$$

The electrostatic potential at any point can be determined by solving the following Poisson equation [44]:

$$\nabla^2 \Phi = -\frac{F}{\varepsilon_0 \varepsilon_r} \sum_{k=1}^{N} z_k C_k \tag{4}$$

where $\varepsilon_0 = 8.854 \times 10^{-12}$ C V^{-1} m^{-1} is the permittivity of a vacuum, $\varepsilon_r = 78.3$ is the relative permittivity of water at temperature 25 °C. Note that Eq. (4) is the constitutive law relating the space-variation in the electric to the charge distribution. In literature most of the work utilised the electro-neutrality condition ($\sum_{k=1}^{N} z_k C_k = 0$) to replace Eq. (4) [20–39]. It is obvious from Eq. (4) that, if the electro-neutrality holds then Eq. (4) can be simplified as $\nabla^2 \Phi = 0$. This implies that if the problem is one-dimensional then the electric field

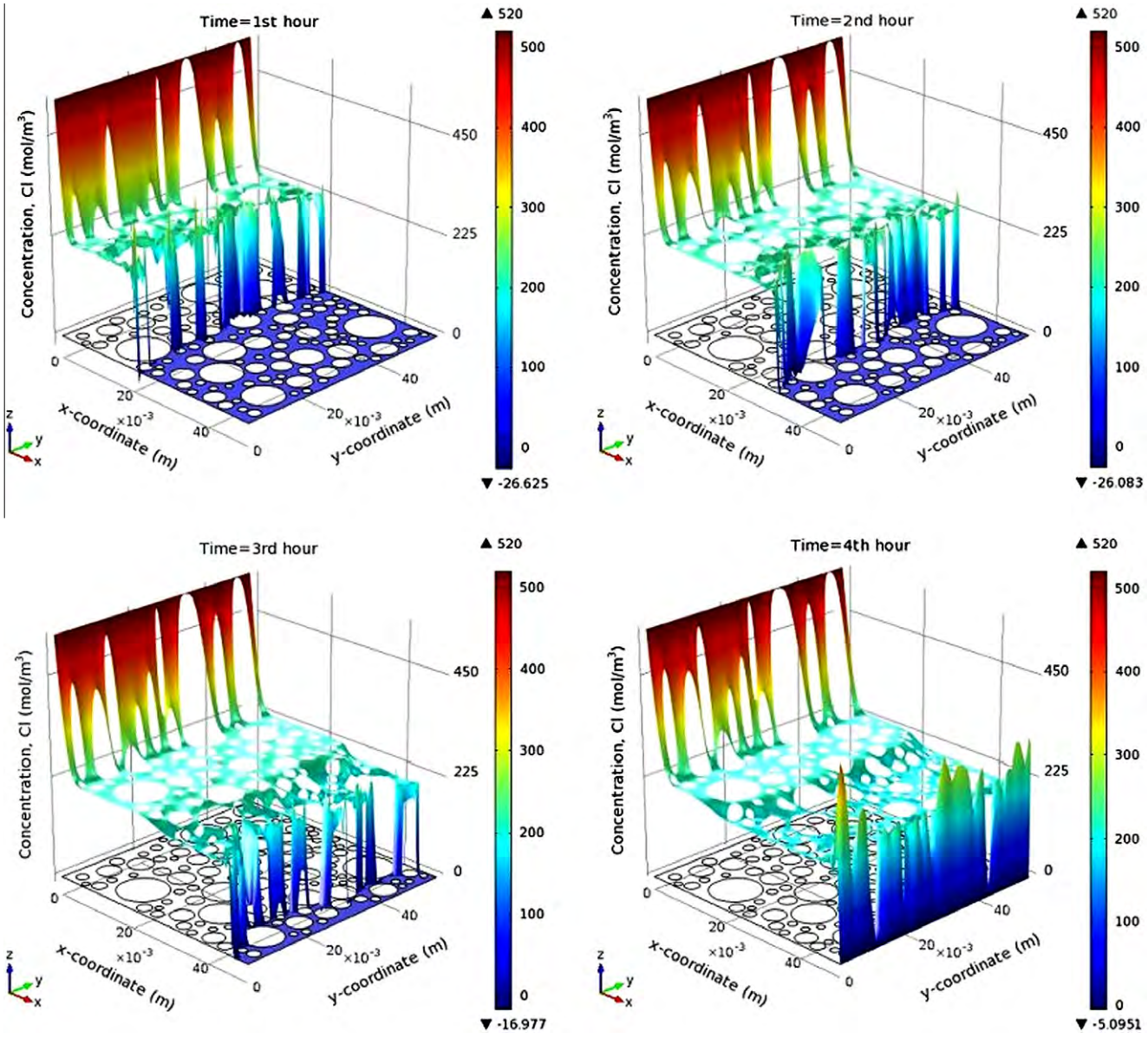

Fig. 6. Concentration distribution profiles of chloride ions.

would be a constant. Numerical examination of Eq. (4) shows that, the constant factor in the right-hand-side of Eq. (4), $\frac{F}{\varepsilon_0 \varepsilon_r}$, is a very large number with the order-of-magnitude of 10^{14}. In order that the left-hand-side of Eq. (4) be finite, the concentration terms in the right-hand-side of Eq. (4) must be very small, i.e. $\sum_{k=1}^{N} z_k C_k \approx 0$. This indicates that the electro-neutrality is not a physical condition but is only a numerical approximation. It should be pointed out here that, $\sum_{k=1}^{N} z_k C_k = 0$ and $\sum_{k=1}^{N} z_k C_k \approx 0$ are qualitatively different although from a numerical point of view these two may be very close. The former implies $\nabla^2 \Phi = 0$ while the latter is not. The governing Eqs. (3) and (4) can be used for solving the concentrations C_k and electrostatic potential Φ if initial and boundary conditions are properly defined.

3. The simulation of migration tests

3.1. Geometry

A set of two-dimensional concrete numerical models with various shapes and volume fractions of coarse aggregates are developed to simulate the migration tests of ionic species in concrete specimens. Fig. 1 shows one of the models adopted in this simulation, which is for the volume fraction of aggregates being $(1 - \phi) = 0.5$ (where ϕ is the 'porosity' of the geometrical model). In the present simulation, the concrete is treated as a heterogeneous composite structure with two phases, in which all circular areas represent the coarse aggregates and the rest is the mortar. The size of the plain concrete is 50×50 mm. The location of the aggregates was randomly generated using a MATLAB program. In reality, the shape of aggregates may not be perfectly circular. However, according to the previous research [7], the influence of particle shapes on the properties of concrete seems not very significant. Therefore, for simplicity, only the concrete model with circular aggregate inclusion is examined here.

It should be also pointed out that, the aggregates in the two phases shown in Fig. 1 are assumed to be impermeable and thus Eqs. (1)–(4) are applied only to the mortar phase, which includes both mortar and interface transition zone (ITZ). This means that all parameters employed in the equations are referred to the composite of the mortar and ITZ. For example, the ionic concentration is the concentration of ions in unit volume of the composite

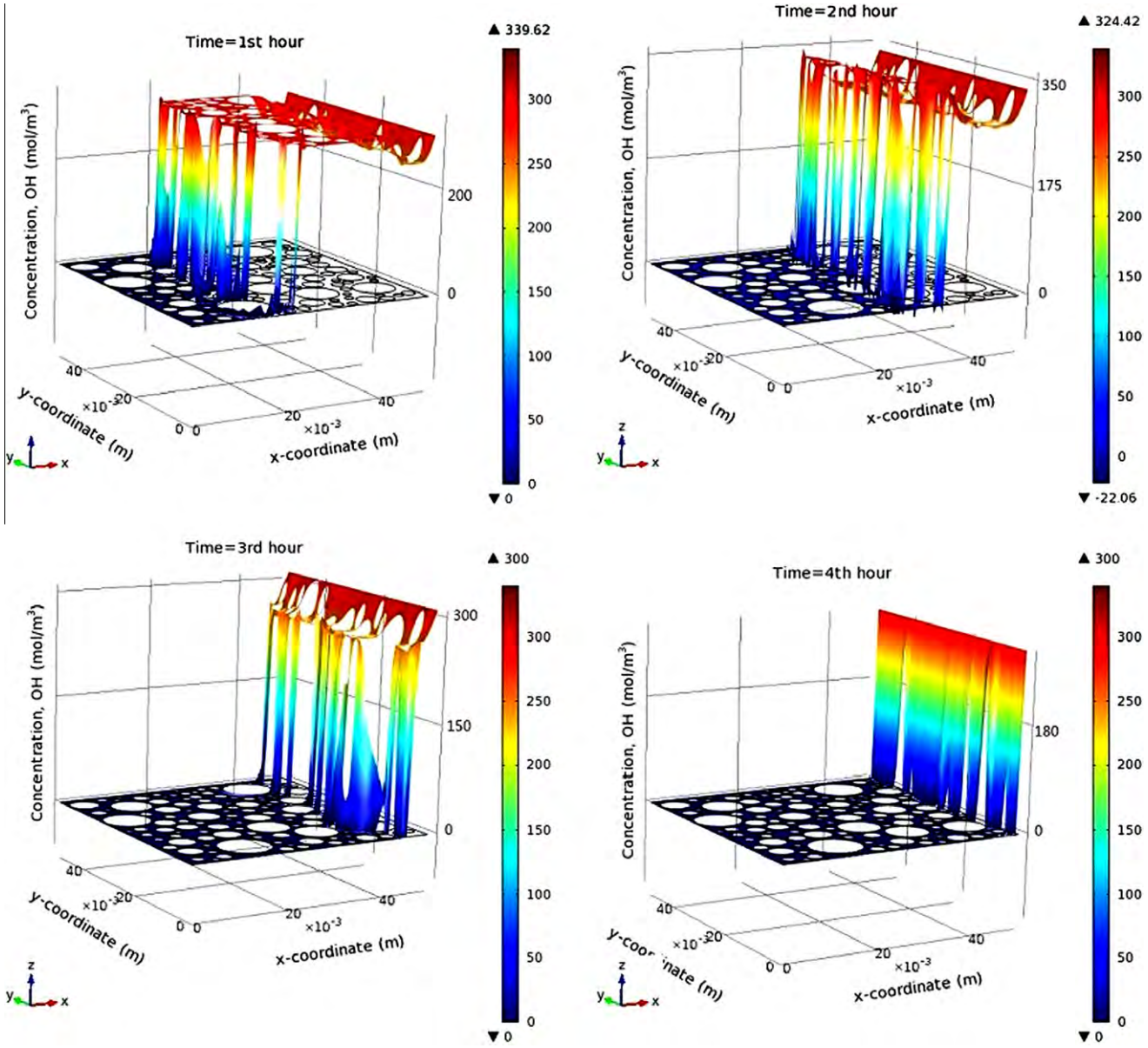

Fig. 7. Concentration distribution profiles of hydroxide ions.

(mortar and ITZ) and the diffusion coefficient is the apparent diffusion coefficient of ions defined in the composite [7] rather than in the pore solution.

3.2. Numerical simulation

The numerical model is used to simulate an 8-h migration test, in which the plain concrete specimen of 50 × 50 mm is located between two compartments, one of which has a 0.52 mole/L NaCl solution, the other of which has a 0.30 mole/L NaOH solution. Externally, there is a 24 V DC voltage applied between two electrodes inserted into the two compartment solutions. The concrete specimen is saturated with a solution of four ionic species (K, Na, Cl and OH) at the initial time. Other ionic species (such as calcium and sulphate) may also exist in the concrete. However, due to their concentrations that are much lower than the four ionic species, only K, Na, Cl and OH are considered in the present simulations. Since the volume of either compartment is much greater than the pore volume of the concrete specimen, it is reasonable to assume that the concentration of each ionic species in the two compartments remains constant during the migration test. In other words, the compartments act like two reservoirs as shown in Fig. 2. The diffusion coefficients of individual ionic species, and the initial and boundary conditions of variables used in the model are given in Table 1, respectively.

3.3. Finite element meshing

Fig. 3 shows the finite element mesh employed in the model, in which the mesh is applied only to the mortar since the aggregates are impermeable and therefore they are not included in the model.

Note that, the accuracy of the numerical solution of the convection-diffusion equation governed by Eqs. (3) and (4) is highly dependent upon the element sizes used. Mathematically, to achieve a reasonably accurate numerical solution, one has to make the Peclet number (produced by the ratio of the diffusion time h^2/D to the convection time h/u, where h is the element size, u is the convection velocity, and D is the diffusion coefficient) to be less

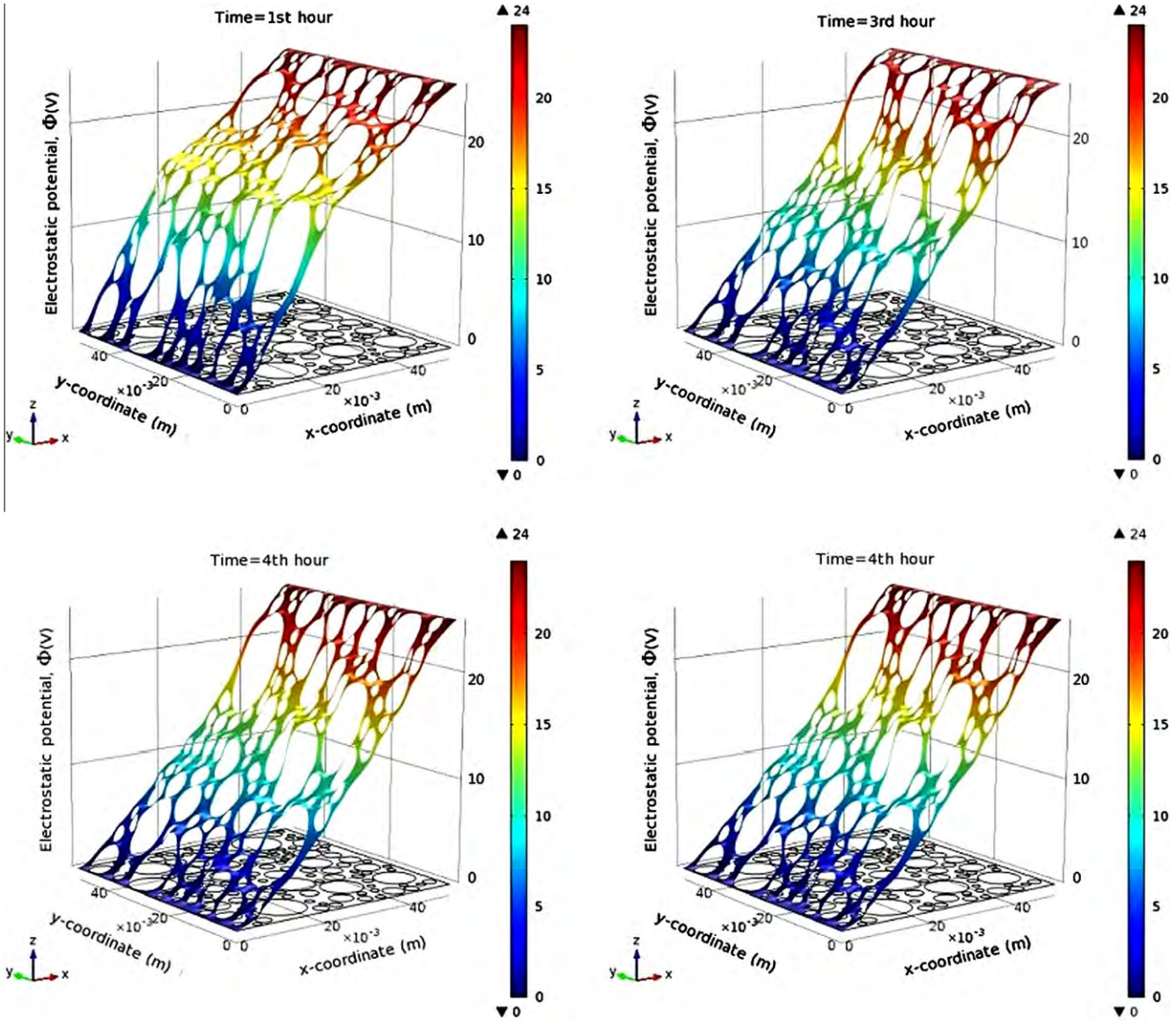

Fig. 8. Electrostatic potential distribution profiles.

than one. Hence, the larger the convection velocity, the smaller the element size required. In the present problem, the convection velocity is the migration velocity of ionic species. When there is an external electric field, the transport of ions in the electrolyte is usually dominated by the migration. In this case the element size must be very small. Otherwise, the numerical solution obtained might not be convergent.

3.4. Simulation results

For given initial and boundary conditions, Eqs. (3) and (4) are numerically solved by using a commercial software COMSOL. Due to the nature of the geometry, the generation of the mesh was controlled by the size of the largest element, which is calculated based on an average value of electrostatic potential gradient (i.e. $\nabla\Phi = \Delta\Phi/L = 480$ V/m). Figs. 4–8 show the distribution profiles of five field variables (the concentrations of four ionic species and the electrostatic potential) obtained at four different times, in which the two plane coordinates represent the position of the variable in the two-dimensional concrete model and the vertical coordinate is the value of the variable (concentration or electrostatic potential). Each frame of individual variable represents one instantaneous moment from the first hour to the fourth hour.

It can be seen from Figs. 4–8 that, during the electro-process the positively charged ions (both potassium and sodium) move towards the cathode, while the negatively charged ions (both chloride and hydroxide) move towards the anode, although the travel speeds of individual ionic species are different. The three-dimensional plots provide a good overall view on the evolution of transport of four ionic species in the specimen due to the influence of an externally applied electric field. It can be observed from the figures that the ionic transport takes place mainly in the x-axis direction due to the influence of the externally applied electric field. In contrast, the ionic transport in the y-axis direction occurs only locally and it is mainly attributed to the tortuosity influence owing to the existence of aggregates.

In order to make a quantitative plot for each ionic species at a given time, one may still prefer to use the traditional two-dimensional plot that is usually used in one-dimensional models. Fig. 9 shows the variation of chloride concentration along the y-axis in sections with given x values at four different times. Note that

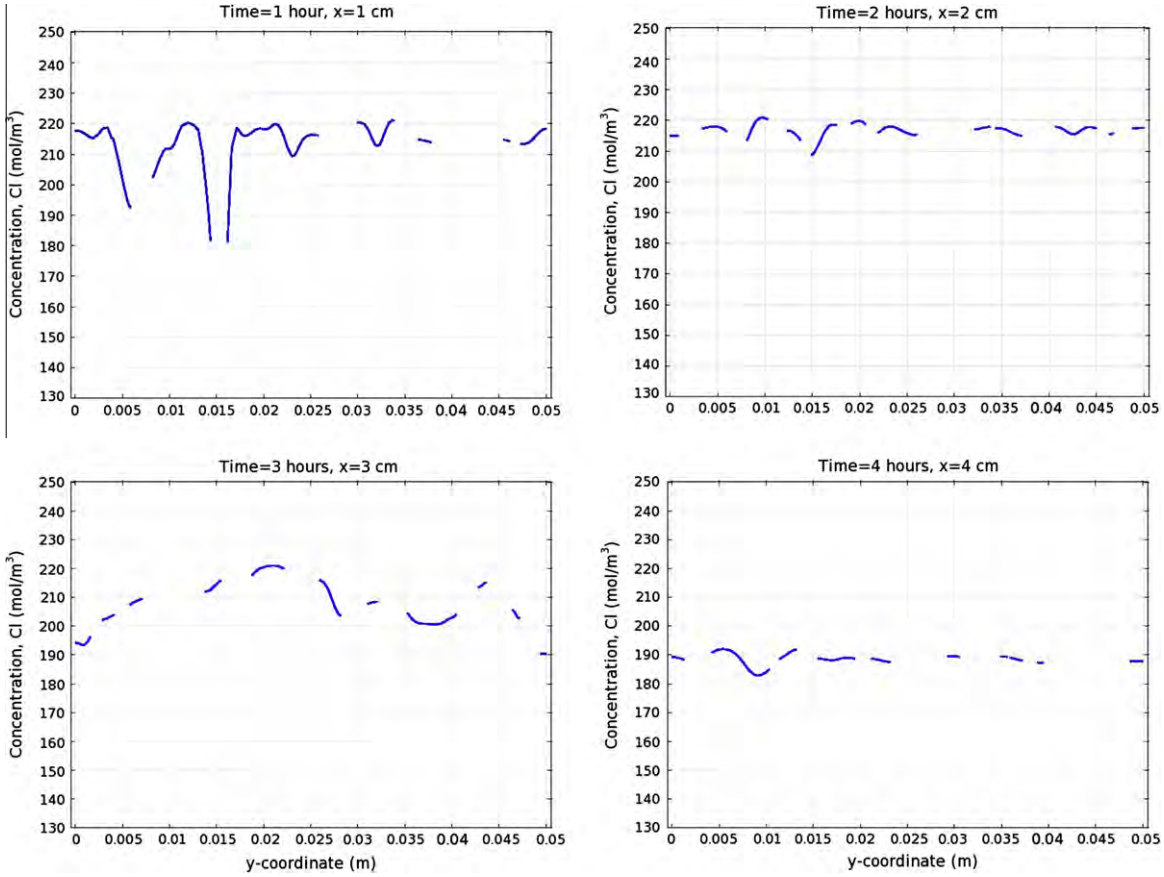

Fig. 9. Section plot of chloride concentration distribution profiles at four different times.

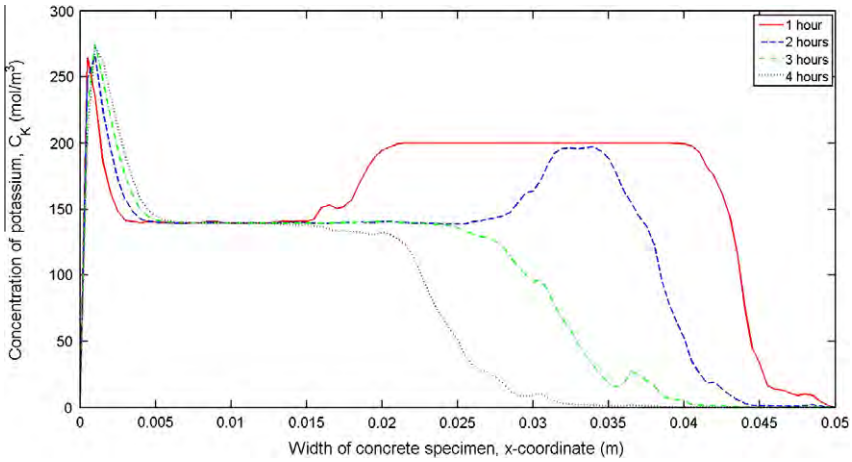

Fig. 10. Overall concentration distribution profiles of potassium ions.

due to the existence of aggregates the concentration is not continuous. Also due to the local influence of the size and position of aggregates the concentration varies irregularly. Nevertheless, overall, this kind of variation seems not very significant, particularly when compared to its variation along the x-axis, as is shown in Figs. 4–8. The reason for this is likely due to the 'sealed' boundary conditions employed at $y = 0$ and $y = L$ boundaries, which make the transport of ions take place almost in one direction. Similar features were found for the other four field variables and thus they are not presented here.

Since the variations of ionic concentrations and electrostatic potential along the y-axis are very small, we can use their average values in the y-direction, i.e. $\bar{z}(x) = \frac{1}{L}\int_0^L z(x,y)dy$ to replace $z(x,y)$ for each field variable. In this case we can re-plot Figs. 4–8 in a two-dimensional format, which are shown in Figs. 10–14.

As is to be expected, due to the effect of aggregates, the distribution curve of ionic concentration or electrostatic potential in the two-dimensional plot shown in Figs. 10–14 is not very smooth in some places. Also, it can be seen from Figs. 10–13 that, the transport behaviour of potassium, sodium and chloride ions is quite dif-

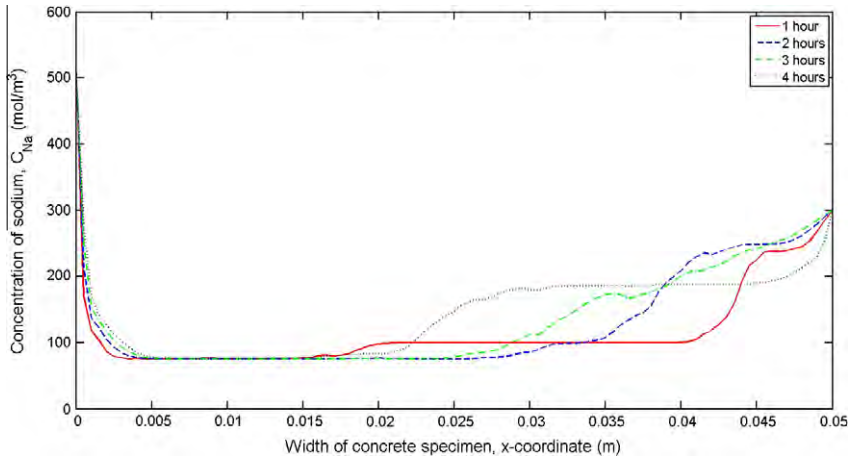

Fig. 11. Overall concentration distribution profiles of sodium ions.

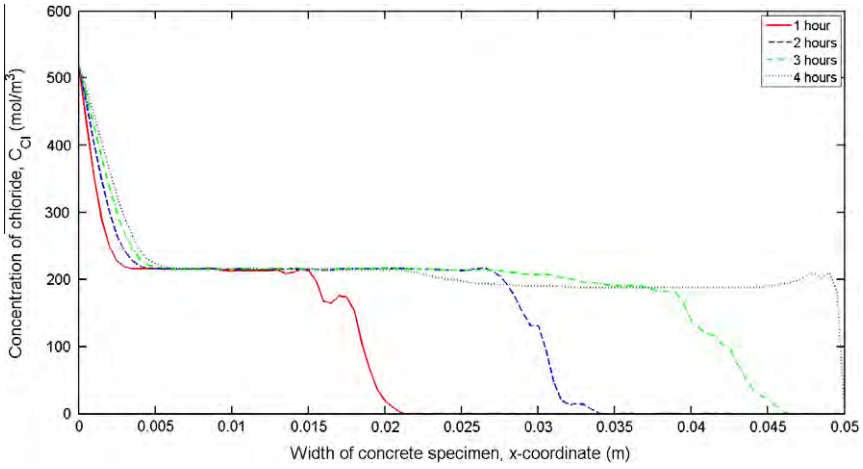

Fig. 12. Overall concentration distribution profiles of chloride ions.

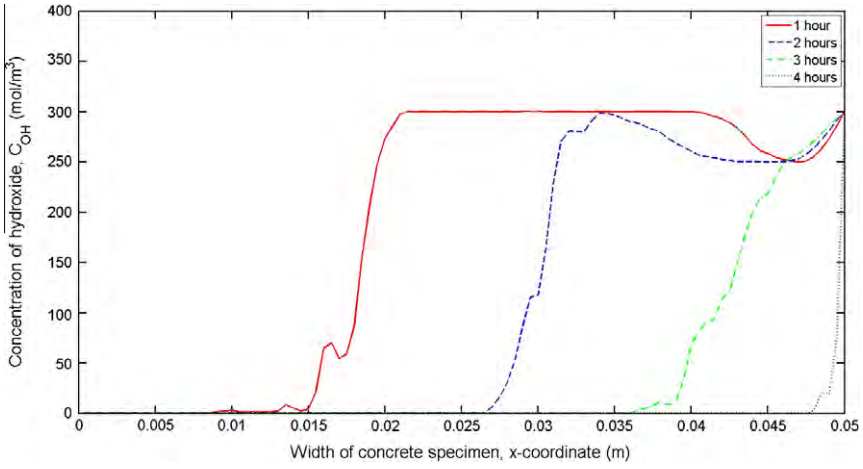

Fig. 13. Overall concentration distribution profiles of hydroxide ions.

ferent from that of hydroxyl ions. The former has a clear diffusion layer in the region near the cathode and a clear migration wave front. The latter has only the migration wave front. For hydroxyl ions, migration is dominant in most of the time. For the other three ionic species, however, diffusion is also very important. This is demonstrated by the migration wave front line that is not very steep (particularly after 2 h). The steep degree of the migration wave front is found to be different for different ionic species, and also for different times. The hydroxyl ions are found to have the steepest wave front, whereas the sodium ions have the gentlest

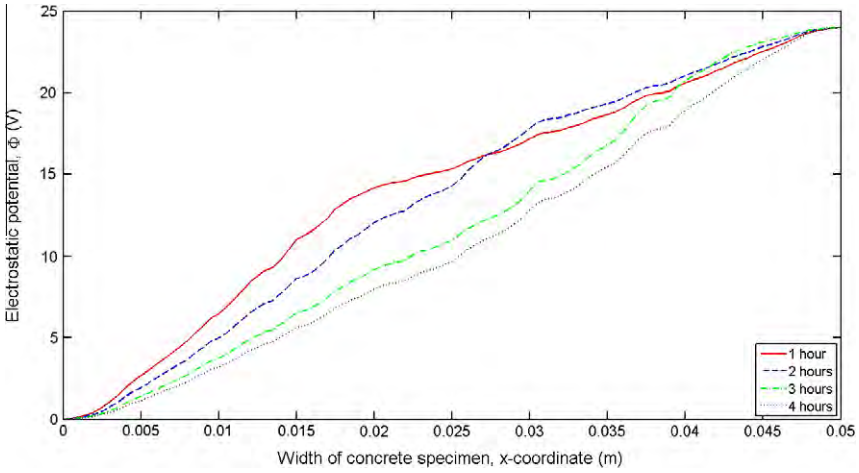

Fig. 14. Overall electrostatic potential distribution profiles.

Table 2
Total amount of ions in the specimen (unit thickness).

Species	Time				
	Initial (mole/m)	1st hour (mole/m)	2nd hour (mole/m)	3rd hour (mole/m)	4th hour (mole/m)
Potassium	0.500	0.385	0.301	0.233	0.181
Sodium	0.250	0.294	0.323	0.342	0.366
Chloride	0	0.215	0.345	0.468	0.537
Hydroxide	0.750	0.463	0.275	0.106	0.010
Total amount	1.500	1.358	1.247	1.150	1.094

wave front. The decrease of steepness with time in the concentration profiles reflects the combined influence of diffusion and local tortuosity. This feature was not found in the single phase model and it is likely due to the inclusion of aggregates in the two-phase model, which provides a direct influence of tortuosity on ionic diffusion and migration.

Careful examination of Figs. 10–13 indicates that the wave speeds of positively (or negatively) charged ions are almost the same but are significantly different from those of their opposite charged ions. This again demonstrates that the electrostatic potential gradient is not constant but regionally dependent. It can be seen from Figs. 10–13 that, as time goes on, the amount of sodium and chloride ions rises, whereas that of potassium and hydroxyl ions reduces in the concrete specimen. The former is due to the boundary conditions, which supply sodium ions and chloride ions from the anode and cathode, respectively. In contrast, the supply of potassium ions from the cathode and hydroxyl ions from the anode does not affect the internal transport of these ions. It is also observed from Figs. 10–13 that, the rate of the increase of sodium and chloride ions in the specimen is lower than that of the decrease of potassium and hydroxyl ions. The reason for this is probably due to the lower diffusion coefficients of the sodium and chloride ions than those of potassium and hydroxyl ions. Table 2 shows a quantitative comparison of the total mole numbers of each ionic species remaining in the specimen at different times. It is evident from the

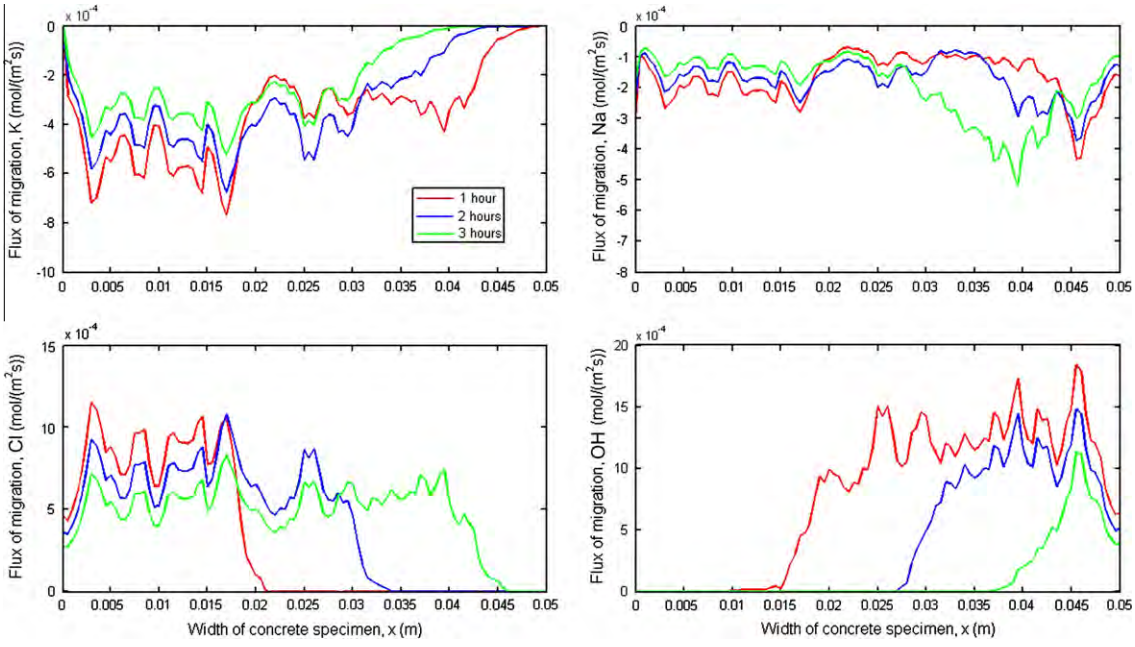

Fig. 15. Distribution profiles fluxes for migration of four ionic species.

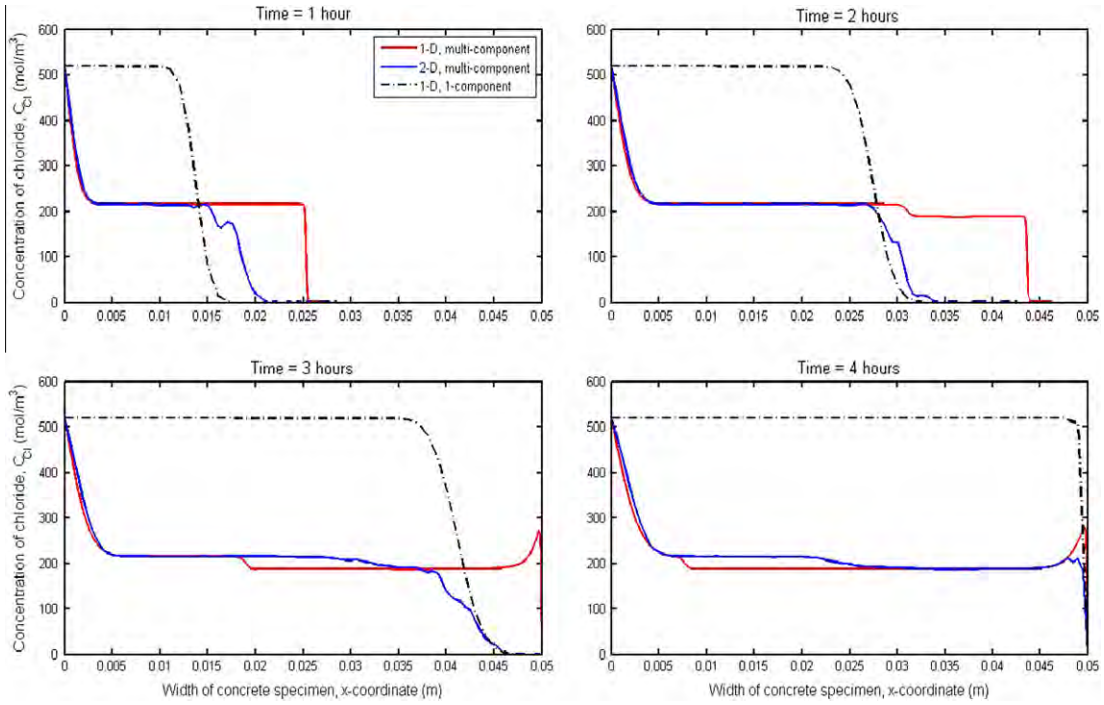

Fig. 16. Comparisons of chloride concentration profiles between three cases.

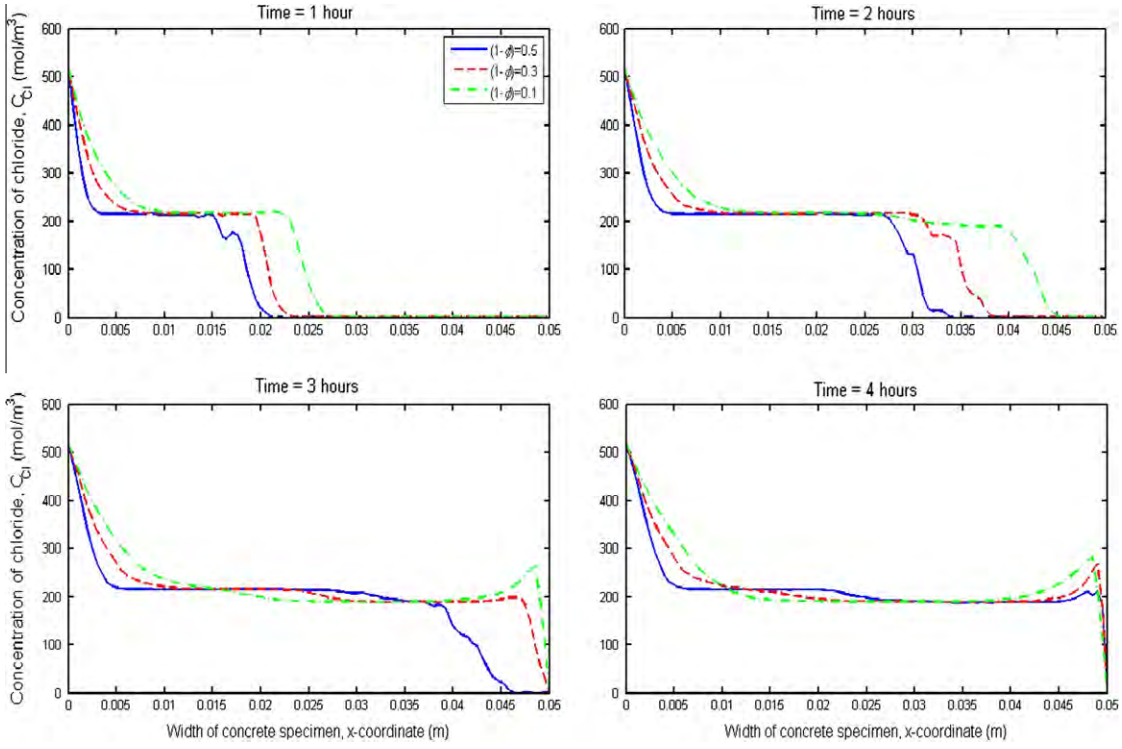

Fig. 17. Influence of aggregate volume fraction on the transport of chloride ions ($1 - \phi$ represents the volume fraction of aggregates).

table that, while the sum of negatively charged ions is balanced by that of positively charged ions, the total quantity of all ions in the specimen is indeed decreasing with time.

It can be seen from Fig. 14 that, the electrostatic potential increases from $\Phi = 0$ at the cathode to $\Phi = 24$ V at the anode, but the increase is not completely linear. It is interesting to notice from the electrostatic potential plot shown in Fig. 14 that the electrostatic potential curve varies from a convex shape at the first hour to a concave shape at the fourth hour. This means that, initially the higher migration speed of ionic species is in the region near

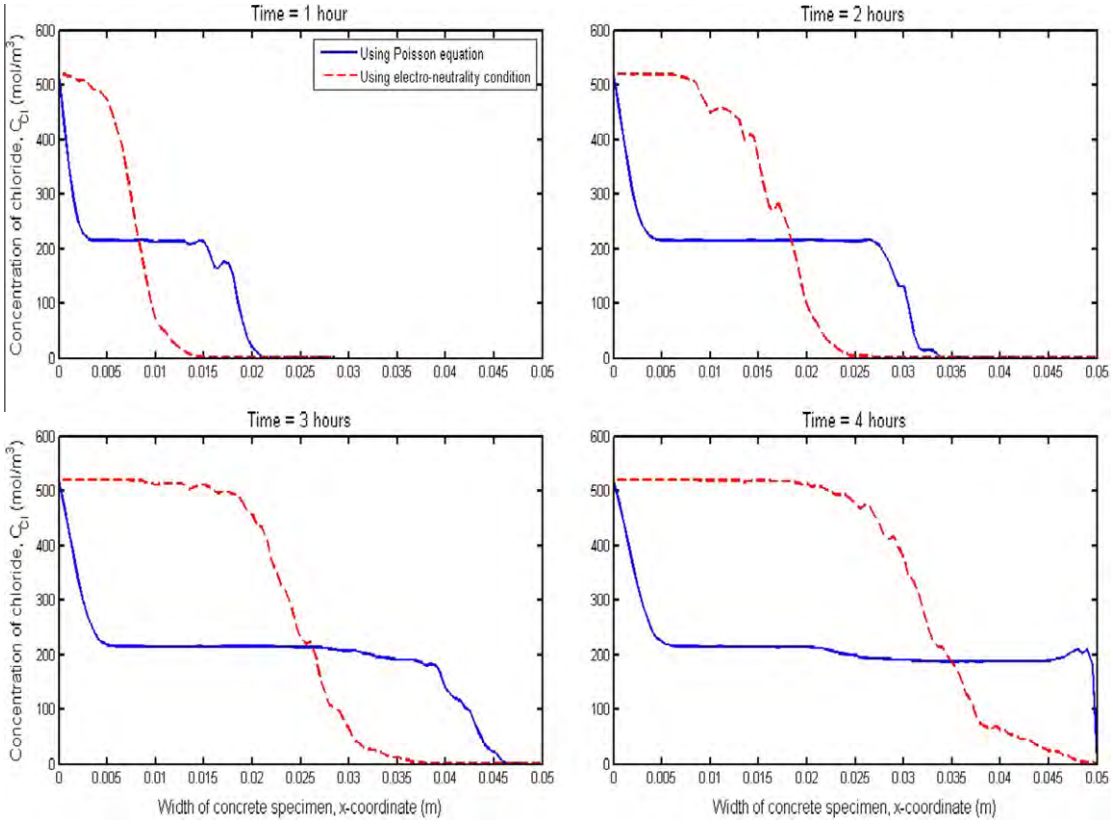

Fig. 18. Comparison of chloride concentration distribution profiles obtained with and without using Poisson's equation.

the cathode, but with time the higher migration speed gradually shifts to the region near the anode. This further demonstrates that migration speed is not constant but varies not only in time but also regionally.

To further demonstrate the variation of migration speed, Fig. 15 shows the migration fluxes of each ionic species at various different times. It is evident from the figure that the migration fluxes of ionic species vary not only with space but also with time, and most importantly they do not follow a single pattern. Of particular interest is the migration of chloride ions, as the diffusion coefficient in the chloride rapid migration test is calculated based on the migration profile. Fig. 16 shows a comparison of chloride concentration profiles at four different times obtained from the present two-dimensional, two-phase, multi-component model, the one-dimensional, single-phase, multi-component model [45], and the one-dimensional, single-phase, one-component model. Interestingly, the two multi-component transport models provide very similar concentrations, but have significantly different travel speeds; the one-dimensional model produces higher travel speed than the two-dimensional model does. In contrast, the one-component model provides higher concentration than the two multi-component models do. However, in terms of the travel speed the one-component model and the two-phase model are closer. This indicates that the interaction between ionic species and the multi-phases are equally important.

In order to examine the influence of the volume fraction of aggregates on the ionic transport, particularly the chloride ions, Fig. 17 shows the concentration distribution profiles of chloride ions at four different times for three different aggregate volume fractions $(1-\phi)$. It can be seen from the figure that, the smaller the aggregate volume fraction, the quicker the chloride ions can travel. The reason for this is likely due to the effect of tortuosity. As the higher the aggregate volume fraction, the larger the tortuosity; therefore, the slower the ionic transport. This is also consistent with what was shown in Fig. 16 and reported in literature [7,9]. However, here it should also be pointed out that, the increase in quantity of aggregates will inevitably increase the ITZ volume in the mortar, which can increase the diffusivity of the concrete [46]. Nevertheless, since the present model does not include the ITZ this kind of effects was not reflected in the results.

To demonstrate the importance of using Poisson's Eq. (4), Fig. 18 shows a comparison of concentration profiles of chloride ions, obtained with and without using Poisson's equation. It can be seen from the figure that, the concentration profiles obtained by using an electro-neutrality condition are quite different from those using the Poisson's Eq. (4). The reason for this is because when the electro-neutrality condition was used, there would be no electro-static potential coupling and therefore the transport of individual ionic species would be independent of each other. This is obviously not correct.

4. Conclusions

This paper has presented a numerical investigation on the transport of ionic species in a plane concrete specimen under the influence of an externally applied electric field. The two-phase numerical model has been used to simulate a 4-h ionic migration test. Results of distribution profiles of ionic concentrations and electrostatic potential at different times have been provided. From the present study the following conclusions can be drawn:

(1) Electro-migration is the most important process in the ionic transport in concrete under the influence of an externally applied electric field. However, local diffusion is also very

important, which may have significant influence on the development of migration speed. Different ionic species may have different transport behaviour, depending on their diffusion coefficients as well as their initial and boundary conditions.

(2) The migration speed of each ionic species varies with time and also with space. The migration speeds of positively (or negatively) charged ions are almost the same but are significantly different from those of their opposite charged ions.

(3) The variation of the ionic distribution profiles and the electrostatic potential profiles along the *y*-axis are insignificant. The concentration distribution profiles obtained from the present two-phase multi-component transport model are qualitatively similar to those obtained from the single-phase multi-component transport model, although quantitative difference in results may exist between these two kinds of models, particularly in the travel speed.

(4) During the electro-process, the total amount of ions within the specimen will vary with time. For the migration test case employed in the present study the amount of ions in the specimen is found to decrease with time.

(5) The plot of the distribution of electrostatic potential between the cathode and anode did not show a straight line, but more likely a curve that varies from a convex shape at the first hour to a concave shape at the fourth hour.

(6) The inclusion of aggregates in the model can provide a more accurate influence of tortuosity on both the diffusion and migration of ions.

References

[1] Atkinson A, Nickerson AK. The diffusion of ions through water-saturated cement. J Mater Sci 1984;19:3068–78.

[2] Hobbs DW. Aggregate influence on chloride ion diffusion into concrete. Cem Concr Res 1999;29:1995–8.

[3] Dormieux L, Lemarchand E. Modélisation macroscopique du transport diffusif Apport des méthodes de changement d'échelle d'espace. Oil Gas Sci Technol 2000;55(1):15–34.

[4] Garboczi EJ. Permeability, diffusivity, and microstructural parameters: a critical review. Cem Concr Res 1990;20(4):591–601.

[5] Brakel JV, Heertjes PM. Analysis of diffusion in macroporous media in terms of porosity, a tortuosity and a constrictivity factor. Int J Heat Mass Transfer 1974;17(9):1093–103.

[6] Xu K, Daian JF, Quenard D. Multiscale structures to describe porous media Part II: Transport properties and application to test materials. Transport Porous Med 1997;26(3):319–38.

[7] Li LY, Xia J. A multi-phase model for predicting the effective diffusion coefficient of chlorides in concrete. Construct Build Mater 2012;26(1):295–301.

[8] Caré S, Hervé E. Application of a n-phase model to the diffusion coefficient of chloride in mortar. Transport Porous Med. 2004;56(2):119–35.

[9] Xi Y, Bazant ZP. Modeling chloride penetration in saturated concrete. J Mater Civil Eng 1999:58–65.

[10] AASHTO T 259. Standard method of test for resistance of concrete to chloride ion penetration. Washington: American Association of States Highway and Transportation Officials; 2003.

[11] NT Build 443. Concrete, hardened: accelerated chloride penetration, Nordtest method, Helsinfors; 1995.

[12] Whiting D. Rapid measurement of the chloride permeability of concrete. Public Roads 1981;45(3):101–12.

[13] AASHTO T 277. Standard method of test for rapid determination of the chloride permeability of concrete. Washington: American Association of States Highway and Transportation Officials; 1983.

[14] ASTM C 1202. Standard test method for electrical indication of concrete's ability to resist chloride ion penetration. Philadelphia: American Society for Testing and Materials; 1994.

[15] Andrade C. Calculation of chloride diffusion-coefficients in concrete from ionic migration measurements. Cem Concr Res 1993;23(3):724–42.

[16] Pfeifer DW, McDonald DB, Krauss PD. The rapid chloride permeability test and its correlation to the 90-day chloride ponding test. PCI J 1994;39(1):38–47.

[17] Tang LP, Nilsson LO. Rapid determination of the chloride diffusivity in concrete by applying an electric field. ACI Mater J 1993;89(1):49–53.

[18] AASHTO TP 64-03. Standard method of test for prediction of chloride penetration in hydraulic cement concrete by the rapid migration procedure. Washington: American Association of State Highway and Transportation Officials; 2003.

[19] Yang CC, Cho SW. The relationship between chloride migration rate for concrete and electrical current in steady state using the accelerated chloride migration test. Mater Struct 2004;37(271):456–63.

[20] Elakneswaran Y, Iwasa A, Nawa T, Sato T, Kurumisawa K. Ion-cement hydrate interactions govern multi-ionic transport model for cementitious materials. Cem Concr Res 2010;40(12):1756–65.

[21] Lorente S, Carcasses M, Ollivier JP. Penetration of ionic species into saturated porous media: the case of concrete. Int J Energy Res 2003;27(10):907–17.

[22] Khitab A, Lorente S, Olivier JP. Predictive model for chloride penetration through concrete. Mag Concr Res 2005;57(9):511–20.

[23] Snyder KA, Marchand J. Effect of speciation on the apparent diffusion coefficient in nonreactive porous systems. Cem Concr Res 2001;31(12):1837–45.

[24] Zelinsky AG, Pirogov BY. Numerical simulation of corrosion process with two-step charge transfer mechanism in the $Cu/CuSO_4 + H_2SO_4$ system. Corros Sci 2006;48:2867–81.

[25] Frizon F, Lorente S, Ollivier JP, Thouvenot P. Transport model for the nuclear decontamination of cementitious materials. Comput Mater Sci 2003;27(4):507–16.

[26] Walton JC. Mathematical modeling of mass transport and chemical reaction in crevice and pitting corrosion. Corros Sci 1990;30(8/9):915–28.

[27] Li LY, Page CL. Modelling and simulation of chloride extraction from concrete by using electrochemical method. Comput Mater Sci 1998;9:303–8.

[28] Li LY, Page CL. Finite element modelling of chloride removal from concrete by an electrochemical method. Corros Sci 2000;42(12):2145–65.

[29] Yu SW, Page CL. Computer simulation of ionic migration during electrochemical chloride extraction from hardened concrete. Brit Corros J 1996;31(1):73–5.

[30] Truc O, Ollivier JP, Nilsson LO. Numerical simulation of multi-species transport through saturated concrete during a migration test – MSDIFF code. Cem Concr Res 2000;30(10):1581–92.

[31] Truc O, Ollivier JP, Nilsson LO. Numerical simulation of multi-species diffusion. Mater Struct 2000;33(233):566–73.

[32] Gravano SM, Galvele JR. Transport processes in passivity breakdown—III Full hydrolysis plus ion migration plus buffers. Corros Sci 1984;24(6):517–34.

[33] Wang Y, Li LY, Page CL. A two-dimensional model of electrochemical chloride removal from concrete. Comput Mater Sci 2001;20(2):196–212.

[34] Yaya K, Khelfaoui Y, Malki B, Kerkar M. Numerical simulations study of the localized corrosion resistance of AISI 316L stainless steel and pure titanium in a simulated body fluid environment. Corros Sci 2011;53:3309–14.

[35] Toumi A, Francois R, Alvarado O. Experimental and numerical study of electrochemical chloride removal from brick and concrete specimens. Cem Concr Res 2007;37(1):54–62.

[36] Kubo J, Sawada S, Page CL, Page MM. Electrochemical injection of organic corrosion inhibitors into carbonated cementitious materials: Part 2 Mathematical modelling. Corros Sci 2007;49(3):1205–27.

[37] Friedmann H, Amiri O, Ait-Mokhtar A. Shortcomings of geometrical approach in multi-species modelling of chloride migration in cement-based materials. Mag Concr Res 2008;60(2):119–24.

[38] Krabbenhoft K, Krabbenhoft J. Application of the Poisson–Nernst–Planck equations to the migration test. Cem Concr Res 2008;38(1):77–88.

[39] Narsillo GA, Li R, Pivonka P, Smith DW. Comparative study of methods used to estimate ionic diffusion coefficients using migration tests. Cem Concr Res 2007;37(8):1152–63.

[40] Johannesson B, Yamada K, Nilsson LO, Hosokawa Y. Multi-species ionic diffusion in concrete with account to interaction between ions in the pore solution and the cement hydrates. Mater Struct 2007;40(7):651–65.

[41] Johannesson B, Hosokawa Y, Yamada K. Numerical calculations of the effect of moisture content and moisture flow on ionic multi-species diffusion in the pore solution of porous materials. Comput Struct 2009;87(1–2):39–46.

[42] Johannesson B. Development of a generalized version of the Poisson–Nernst–Planck equations using the hybrid mixture theory: presentation of 2D numerical examples. Transport Porous Med 2010;85(2):565–92.

[43] Johannesson B. Comparison between the gauss' law method and the zero current method to calculate multi-species ionic diffusion in saturated uncharged porous materials. Comput Geotech 2010;37(5):667–77.

[44] Newman JS, Thomas-Alyea KE. Electrochemical systems. third ed. New Jersey: John Wiley & Sons, Inc.; 2004.

[45] Li LY, Xia J. Numerical simulation of ionic transport in cement paste under the action of externally applied electric field. In: Proceedings of international symposium on cement and concrete materials, November 7–9; 2011, Ningbo, China.

[46] Care S. Influence of aggregates on chloride diffusion coefficient into mortar. Cem Concr Res 2003;33:1021–8.